

QUESTION 1 Page 3-1;

What correlation exist between the spectra in Figure 3-1 and Figure 3-2?

RESPONSE

The design response spectra given in Figure 3-1 and Figure 3-2 were identical, but they were plotted on log-log and linear-linear scales, respectively. The response spectrum curve of the synthesized earthquake time history was also given in Figure 3-2 to show the conservative enveloping of the design response spectrum.

8102200415

0222F

QUESTION 2      Page 3-6 and; Q1 question 12

Comparisons between analytical models and experimental results are important. Although the model has not changed, the experimental fit of the model has. Supply quantitative comparable experimental and analytical stress-strain results and a basis for comparison of these results.

RESPONSE

The strain data was obtained at selected thimble locations during the optimized fuel assembly lateral loading test. The test set-up as well as the gage locations is schematically shown in Fig.Q2.1. The thimble stresses derived from the strain reading are shown in Figure Q2.2.

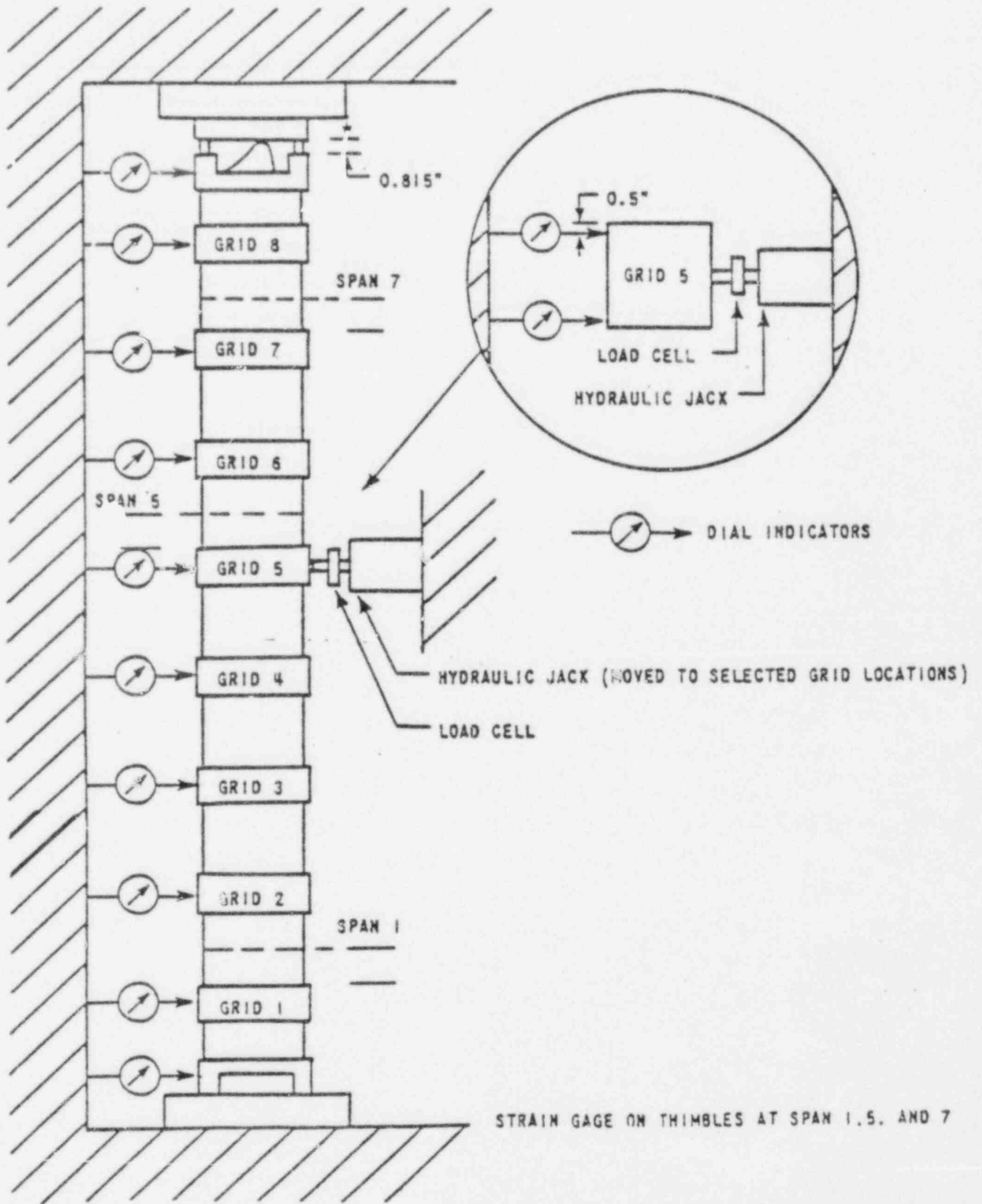


FIGURE Q2.1 17x17 OPTIMIZED FUEL ASSEMBLY LATERAL STIFFNESS TEST SETUP AND STRAIN GAGE LOCATIONS

Bending Stress (psi)

Direct Stress (psi)

Deflection (in)

+b,c

FIGURE Q 2.2 17x17 OPTIMIZED FUEL ASSEMBLY THIMBLE STRESS VERSUS LATERAL DEFLECTION  
EOL COLD

QUESTION 3 Page 3-6;

The discussion concerning the model shown in Figure 3-4 is confusing. Please clarify.

RESPONSE

The lateral fuel assembly finite element model has been experimentally verified for the Westinghouse type fuel design. The discussion of the FEM is documented in WCAP-8236. A brief discussion of the lateral fuel assembly model is presented.

The fuel assembly model consists of the following structural modeling:

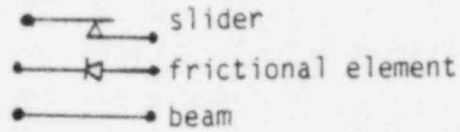
- 1) The fuel assembly skeleton structure which contains an array of twenty-four thimble tubes plus one instrumentation thimble, is represented by a pair of 2D-beam columns. The structural rigidity was established by properly spacing the vertical beams through the use of parallel theorem for calculating the equivalent moment of inertia.

The beam elements were used to simulate fuel nozzles and grid stiffnesses.

- 2) The fuel rods were modeled by two vertical beams. Since the fuel rod lateral deflections are independent of positions within the array, the summation of the individual fuel rod properties was used to simulate all of the rods.
- 3) The grid dimples and springs were modeled using friction elements, which are preloaded linear springs with out of plane friction to simulate the fuel rod lift-off within a grid. The functional elements were also used to model the axial fuel rod drag force in the grid cell.

The side dimples were represented by a slider type element to simulate the frictional effects caused by fuel rods sliding on the side dimple. The slider element is basically a simplified one dimensional frictional element.

The legend for Fig 3-4 is



The element 5-11 in the text should be correctly read as 5-7.

- 4) A schematic representation of a portion of the fuel rod and the grid restraints is shown in Figure Q3.1.

b, c

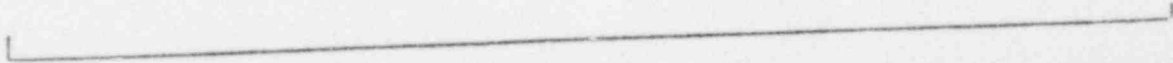


FIGURE Q.1 SCHEMATIC OF A FUEL ROD WITH GRID RESTRAINTS

QUESTION 4 Page 3-8;

Provide analytical-experimental correlations for the fuel assembly lateral force-deflection response.

RESPONSE

The experimental-analytical correlations for the Westinghouse type fuel assembly design were documented in WCAP-8236. The fuel assembly lateral load versus deflection responses for the 17x17 OFA is shown in Fig Q4.1.



FIGURE Q4.1 17x17 OPTIMIZED FUEL ASSEMBLY LOAD VERSUS DEFLECTION -  
LOAD APPLIED AT GRID NO. 5 - EOL COLD

QUESTION 5

[ ]<sup>†</sup> is important in predicting core plate motion. Provide additional detail showing how this effect was implemented and what analytical-experimental justification exists for its use. Supply this information for both the lateral and vertical implementation. (a,c)

RESPONSE

[ ]<sup>†</sup> is included for LOCA evaluation in the MULTIFLEX thermal hydraulic computer code. MULTIFLEX documentation is provided by Reference 5 of WCAP-9401. (a,c)

For seismic evaluation, [ ]<sup>†</sup> representation was included in the reactor vessel structural model to more accurately represent the reactor vessel structural dynamics in a [ ]<sup>†</sup>. The outputs of the seismic analysis of the reactor vessel model are lateral core plate motions and fuel assembly vertical nozzle loads. (a,c)

[ ]<sup>†</sup> (a,c)

$^{+}(a,c)$

$^{+}(a,c)$

$\Gamma^+(a, c)$

$^+(a,c)$

$^+(a,c)$

TABLE A

COMPARISON OF VERITICAL MODEL RESULTS WITH EXPERIMENTAL DATA

A large, empty rectangular frame with a thin black border, intended for a table. The frame is positioned centrally on the page, below the title and above the footnote.

<sup>+</sup>(a,b,c)

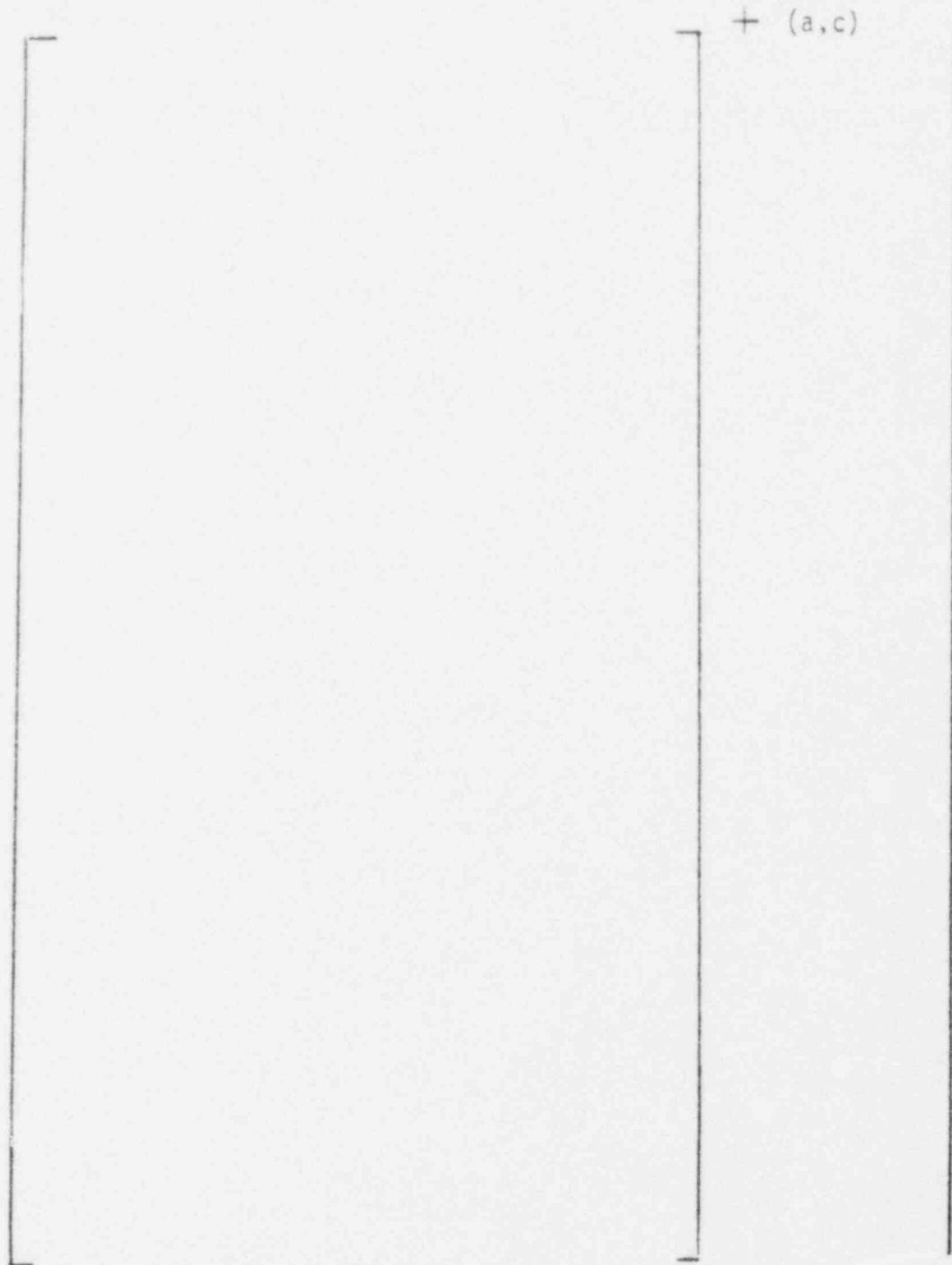


Figure 3-7(b) Reactor Core Barrel Model

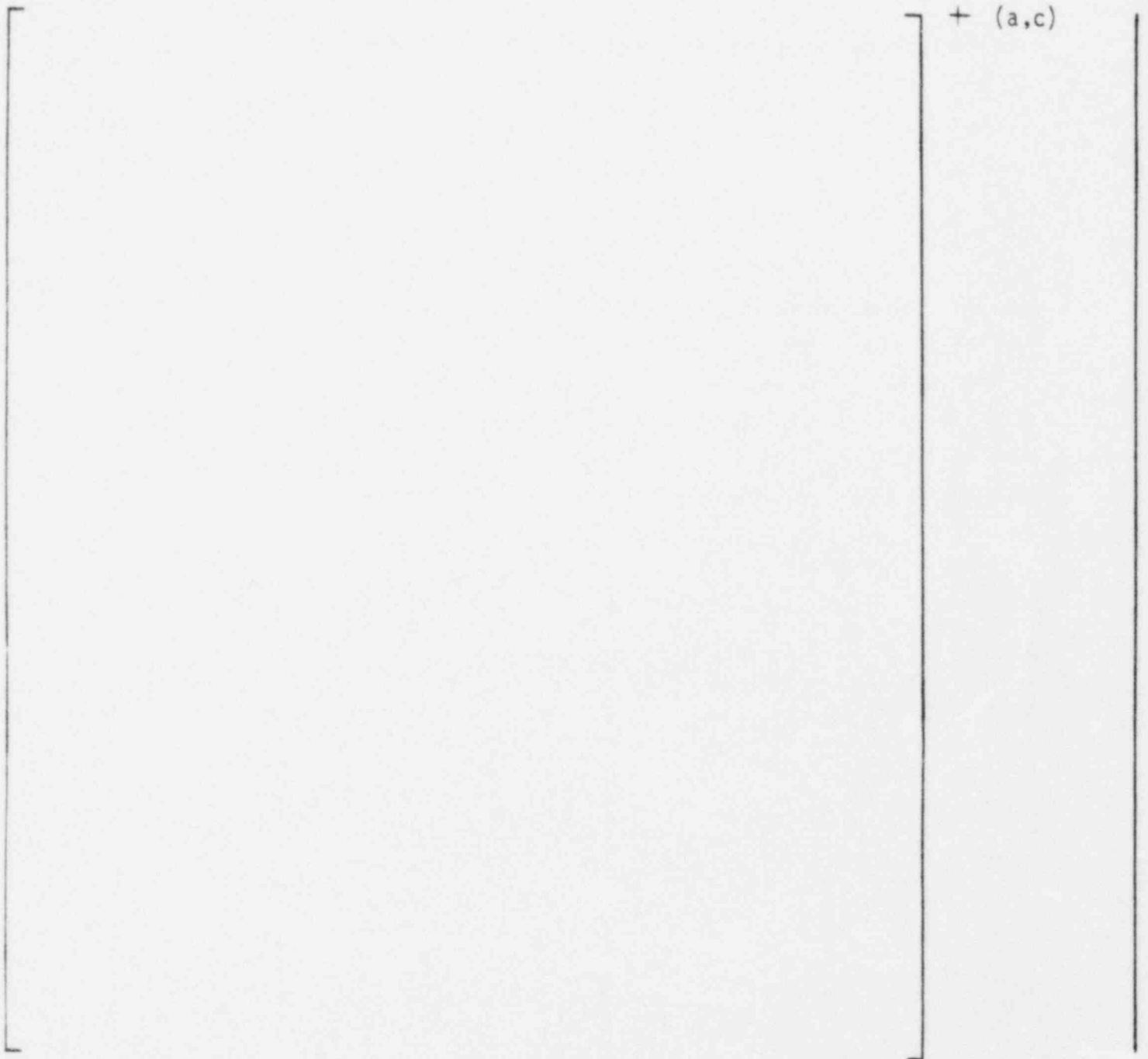


Figure 3-7(d) Vertical Hydrodynamics Model

QUESTION 6 Page 3-19;

Only one spectra is shown in Figure 3-1. Refer to question 1.

RESPONSE

The response spectrum curve given in Fig. 3-1 was developed by enveloping the response spectra for a number of typical Westinghouse four loop neutron panel plants. Since the spectrum presented in Fig. 3-1 is relatively severe, it is judged to be conservative in establishing the fuel capability. For plant designs which could exceed the given spectrum, specific analysis using the plant spectrum may be required.

QUESTION 7 Page 3-20 and; Q1 question 5

The response to Question Set 1 question 5 and the comment presented on page 3-20 concerning the importance of the fuel assembly fundamental mode of vibration to core region response appear to suggest different points of view. Explain.

RESPONSE

The peak grid impact response is, in general, dependent on the fundamental fuel assembly vibrational frequency. The answer to Question 5 of Q1 suggested that the added water mass tends to lower the fuel assembly fundamental frequency slightly.

QUESTION 8 Page 3-20;

Justify that [ ]<sup>+</sup> is a reasonable way to judge the worst case fuel system loading considering the fuel system response is nonlinear. Which [ ]<sup>+</sup> cases produced the largest impact forces and peak fuel assembly displacements in the system model? Do these cases correspond to the [ ]<sup>+</sup> case chosen?

a,c

a,c

a,c

RESPONSE

Seismic analyses using a number of different seismic waves have demonstrated that the [ ]

[ ]<sup>+</sup>. The selected worst case wave corresponded to the [ ]<sup>+</sup> system. The fuel assembly grid maximum impact forces obtained from the Reactor Internals models generally occurred for the same input waves selected using the response spectra method.

a,c

a,c

The time history designated as case 2 was used to assess the Optimized Fuel Assembly seismic response. As shown in Figure Q8.1, the acceleration response spectrum obtained from the case 2 seismic time history envelopes the response spectra generated for the remaining six seismic waves in the [ ]<sup>+</sup>

] <sup>+</sup>

a,c



+b, c

FREQUENCY (HZ)

FIGURE Q8.1

FREQUENCY RESPONSE SPECTRA AT UPPER CORE PLATE

LEGEND

Case			
1	.....	5	—...—
2	————	6	—...—
3	-----	7	—...—
4	-----		

QUESTION 9 Page 3-21;

Specify the break opening times used in the analyses. Provide additional data to support the break opening times selected.

RESPONSE

Reference 6 of WCAP 9401 specifies the standard break opening times used in Westinghouse LOCA analyses as instantaneous, 1 millisecond. This break opening time was the analytical basis used in WCAP 9401 which has been the NRC's accepted analytical basis.

What maximum percent error from the experimental values is associated with each analytical mode shape and analytical frequency?

RESPONSE

The mode shapes for the fuel assembly detailed model and the lumped mass-spring models were compared with the experimentally determined modes and indicated relatively good agreement. The lumped mass model used in the reactor core analyses is derived using an analytical procedure[

].<sup>†</sup> The natural

a,c

frequencies for the lumped mass model was based on experimental and finite element data with some minor adjustments to reflect operating conditions.

QUESTION 11 Page 3-26;

Are the analytical predictions presented in Figure 3-12 derived from the model values presented in Table 3-1? If not, discuss the differences.

RESPONSE

Yes.

The response given to Question Set 1 question 6 is somewhat confusing. The core region model presented in Figure 3-10 shows the definite inclusion of  $K_S$  and  $C_S$  values. Please supply a short explanation to resolve this situation.

RESPONSE

The in-grid and through-grid stiffnesses as defined by the NRC are associated with the method of grid impact testing. The in-grid dynamic stiffness is normally determined from tests in which a weighted grid is given an initial velocity and is impacted against a rigid or grid restraint. The through-grid stiffness is usually determined from tests in which a rigid mass impacts a stationary grid.

As shown in Fig. 3-10 the grid stiffness properties designated as  $K_g$  and  $C_g$  were obtained from through-grid impact tests at operating temperature. The local grid stiffness properties,  $K_S$  and  $C_S$  which represent the combined flexibility of the grid springs, dimples, and fuel rods, were determined from the fuel assembly lateral impact tests rather than from the in-grid impact tests.

The fuel assembly lateral impact properties such as impact duration, impact force, and rebound, together with the fuel assembly finite element model, were used to obtain  $K_S$  and  $C_S$  values.

QUESTION 13 Page 3-26 and;

The methods used for determining  $K_s$ ,  $C_s$ ,  $K_g$ ,  $C_g$ , and the critical load ( $P_{crit}$ ) have been discussed and information supplied supporting the values derived for the inconel spacer grids. The incorporation of Zircaloy grids in the fuel assembly design will effect the response of the fuel system and certain spacer grid allowable loads. To completely review this situation, the following information is requested:

- a. test data supporting the in-grid stiffness and damping values chosen,
- b. test data supporting the through-grid stiffness and damping values chosen, and
- c. test data supporting the value of  $P_{crit}$  chosen.

When discussing the above test data, discuss the velocities used in the impact test relative to those calculated analytically from the core region response. Discuss static and dynamic test values.

RESPONSE a.

The local grid flexibility (or in-grid stiffness damping values)  $K_s$  and  $C_s$  are derived from the fuel assembly lateral impact tests. The fuel assembly lateral impact test arrangement is shown in Fig. Q13.1. The impact duration obtained from these tests was approximately [ ]<sup>+</sup> sec. A correlation analysis was performed using the lumped mass-spring analytical model to verify the model by comparing the grid impact forces. These results are given in Table Q13.1.

b,c

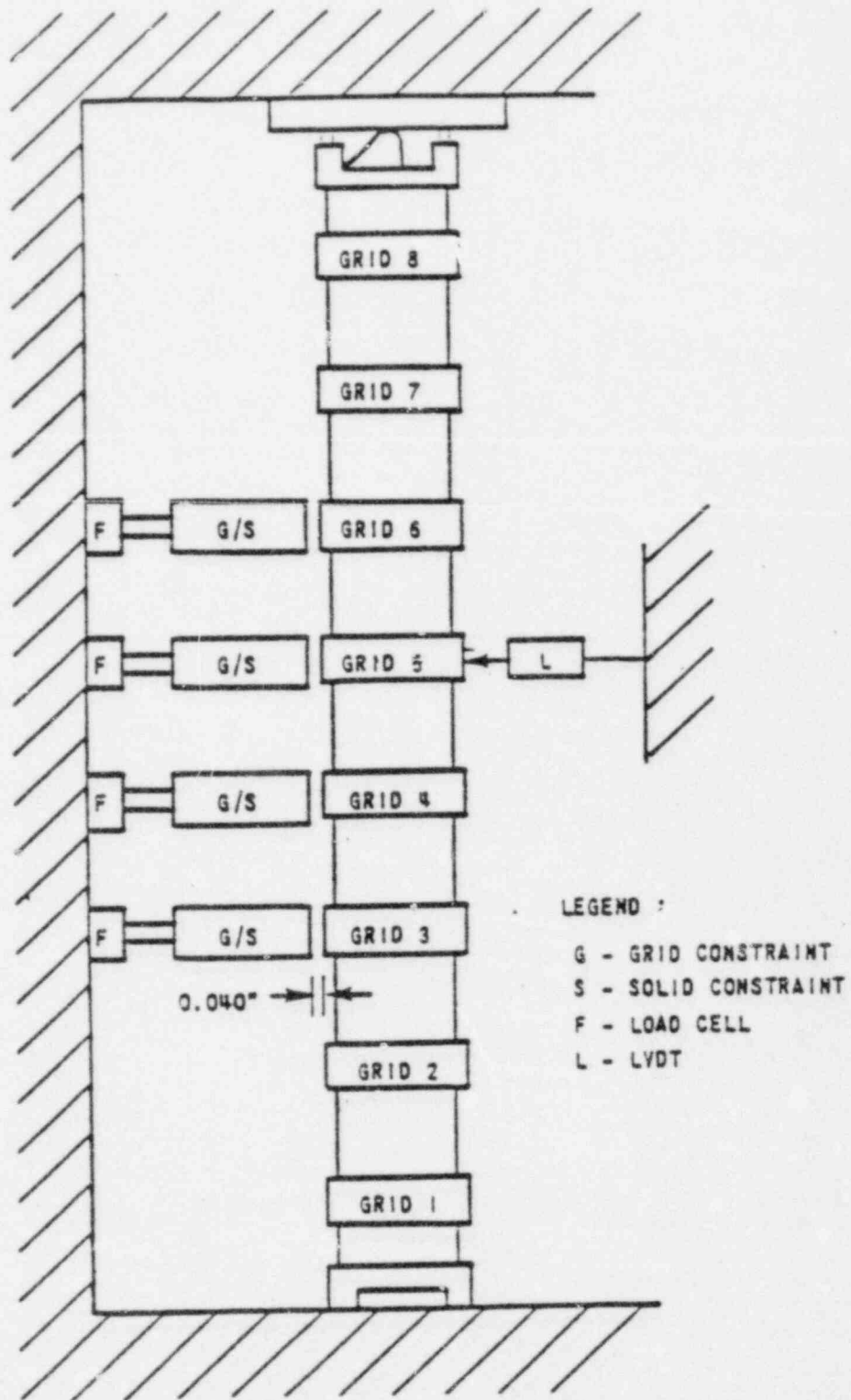


FIGURE Q13.1 17x17 OPTIMIZED FUEL ASSEMBLY LATERAL IMPACT TEST SETUP

TABLE Q13.1

COMPARISON BETWEEN FEM AND FA LATERAL IMPACT RESULTS

(Total Initial Deflection = [ ]<sup>+</sup> in.)

b,c

	FEM	Test	+
Time Duration (sec.)			
Rebound (in.)			b,c
Max. Impact Force (lb)			

RESPONSE b.

The average dynamic through-grid stiffness for the zirc grids tested at [ ]<sup>+</sup>°F using the impact duration method was [ ]<sup>+</sup> lb/in. b,c

This value was determined using energy methods in conjunction with the experimentally determined average impact duration of [ ]<sup>+</sup> sec obtained b,c from the six test samples.

RESPONSE c.

The grid impact force as a function of impact velocity for the six Zircaloy grids tested at [ ]<sup>+</sup>F is shown in Fig. Q13.2. The average crush strength value is [ ]<sup>+</sup> lbs. with a standard deviation of [ ]<sup>+</sup> lbs. b,c  
The lower bound 95 percent confidence limit for the true mean crush strength using a one-tailed statistical analysis for the six samples is [ ]<sup>+</sup> lbs. b,c

The relative fuel assembly velocity plot for grid 4 of a typical peripheral fuel assembly is given in Figure Q13.3. The relative fuel assembly velocity prior to the maximum impact force response is approximately [ ]<sup>+</sup> in/sec, which is consistent with the testing impact velocity. b,c

IMPACT FORCE (LB)

+b,c

IMPACT VELOCITY (IN./SEC)

FIGURE Q13.2 17x17 OFA ZIRCALOY GRID IMPACT FORCE AS A FUNCTION OF VELOCITY AT 600°F

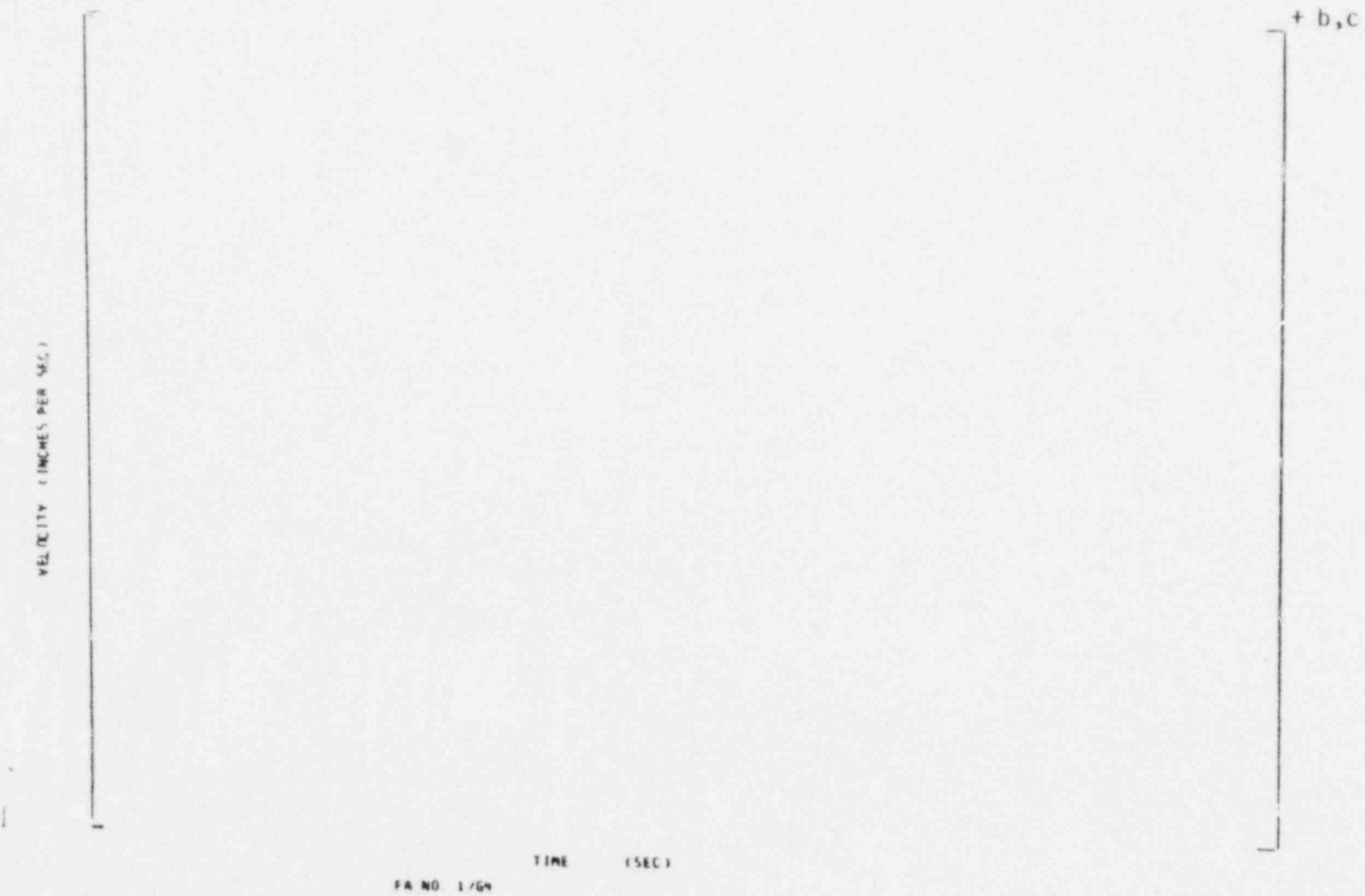


FIGURE Q13.3 RELATIVE VELOCITY - GRID NO. 4 OF A TYPICAL PERIPHERAL FUEL ASSEMBLY

When presenting the above test data, discuss the velocities used in the impact test relative to those calculated analytically from the core region response. Discuss static and dynamic test values.

Supply the value of the friction force per grid which causes fuel rod slippage. Compare beginning-of-life friction values to end-of-life values and discuss the effect these values have on the axial dynamic response of the fuel assembly and resulting critical stresses.

RESPONSE

The average drag force required to cause fuel rod sliding at beginning-of-life (BOL) measured from the demonstration fuel assemblies was [ ]<sup>+</sup> lb. The grid spring force in the zircaloy grid cell is projected to be fully relaxed at end-of-life (EOL) with the drag force estimated to be approximately [ ]<sup>\*\*</sup> lbs. b,c b,c

The fuel assembly axial impact tests simulated the EOL condition and were performed with the internal grid cells pregapped. The test results indicated that the fuel assembly impact force did not exceed [ ]<sup>+</sup> lbs at a drop height up to [ ]<sup>+</sup> inches. The impact force was well below that obtained for a typical BOL fuel assembly, since the sliding of the fuel rod tends to mitigate the fuel assembly axial impact forces. Thus the BOL fuel assembly properties at temperature were incorporated in the reactor internal model for calculating the axial impact responses. b,c b,c

QUESTION 15 Page 3-56;

Supply the fuel assembly location where the data in Figure 3-25 was obtained. How and at what location was the load applied?

RESPONSE

The curves presented in Figure 3-25 were obtained for an axially applied load at the top nozzle. The deflection were measured at the same location and in the same direction as the applied load.

QUESTION 16 Page 3-57;

Drop test data is particularly important in developing an axial dynamic impact model. Supply analytical-experimental drop test correlations and the experimentally derived constant "D" used to calculate the impact damping coefficient.

RESPONSE

A [

b,c

] was incorporated in the axial fuel assembly model. The finite element model was experimentally verified based on drop impact tests. The analytical-experimental correlations for a typical Westinghouse type fuel assembly is shown in Fig. Q16.1 and have been verified by a number of designs.

Question 17: Safe-Shutdown Earthquake (SSE) lateral core plate motions are presented in Figure 3-8, followed by lateral LOCA core plate motions in Figure 3-19. Supply similar information for the vertical applied loads (preferably in the form of pressure time histories at the core inlet and core outlet).

Response: Figures 17-1 through 17-5 represent the vertical forces which were applied to the RPV structural model at the core plates and fuel assemblies. These forces correspond to the [

]<sup>+</sup>

(a,c)

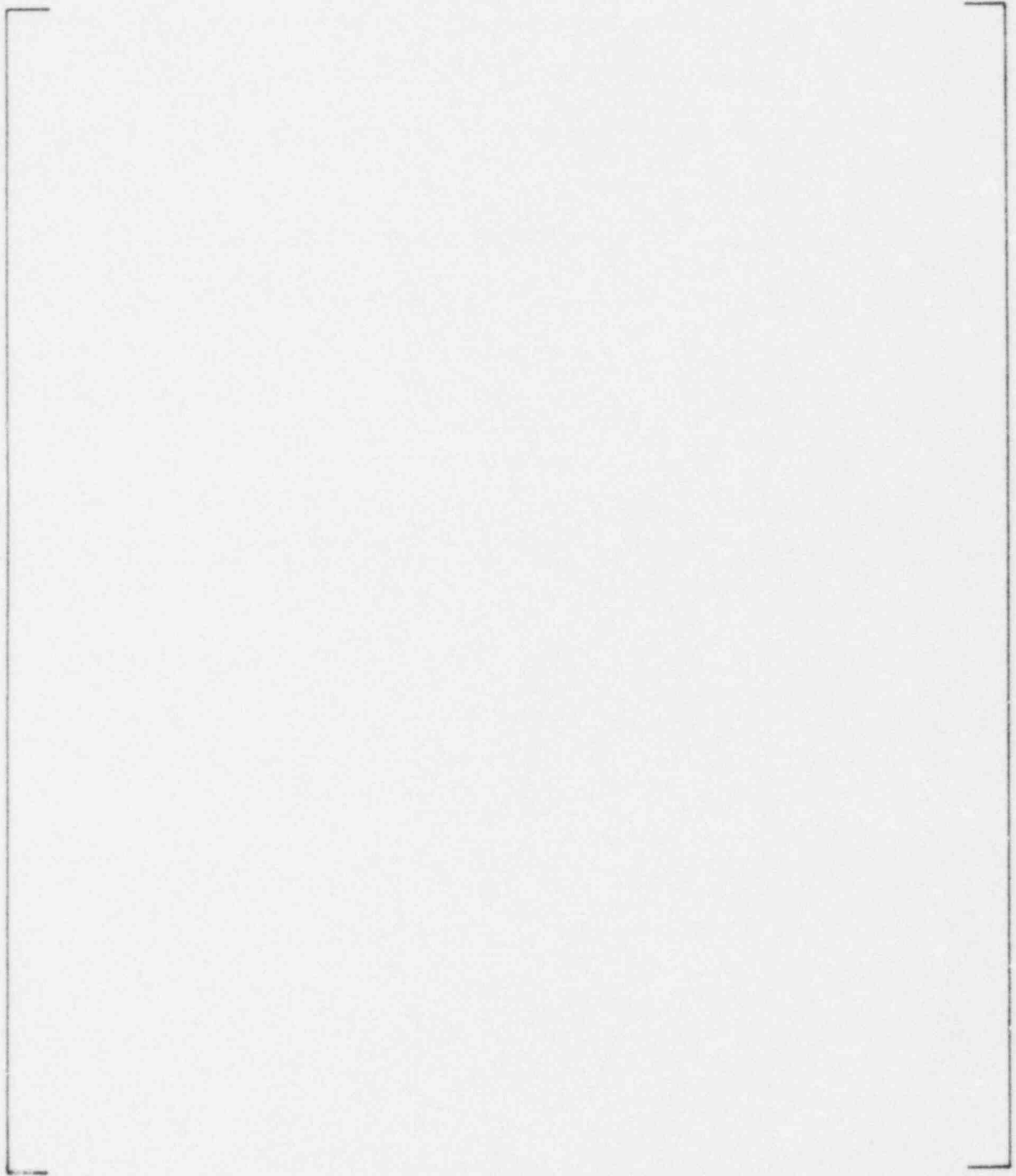


Figure 17-1. Total Vertical Force on Upper Core Plate

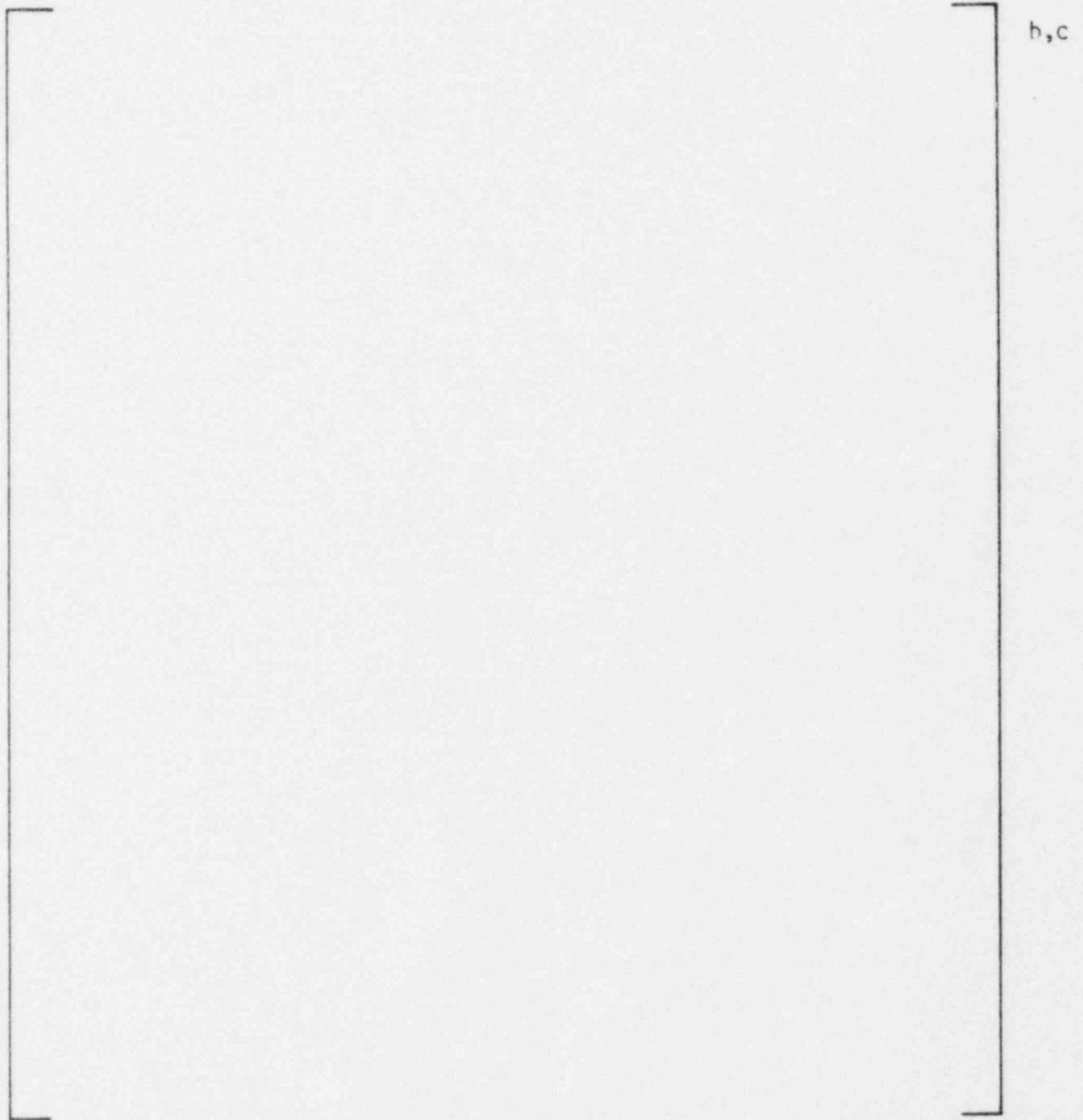


Figure 17-2. Total Vertical Force on Top Fuel Nozzle

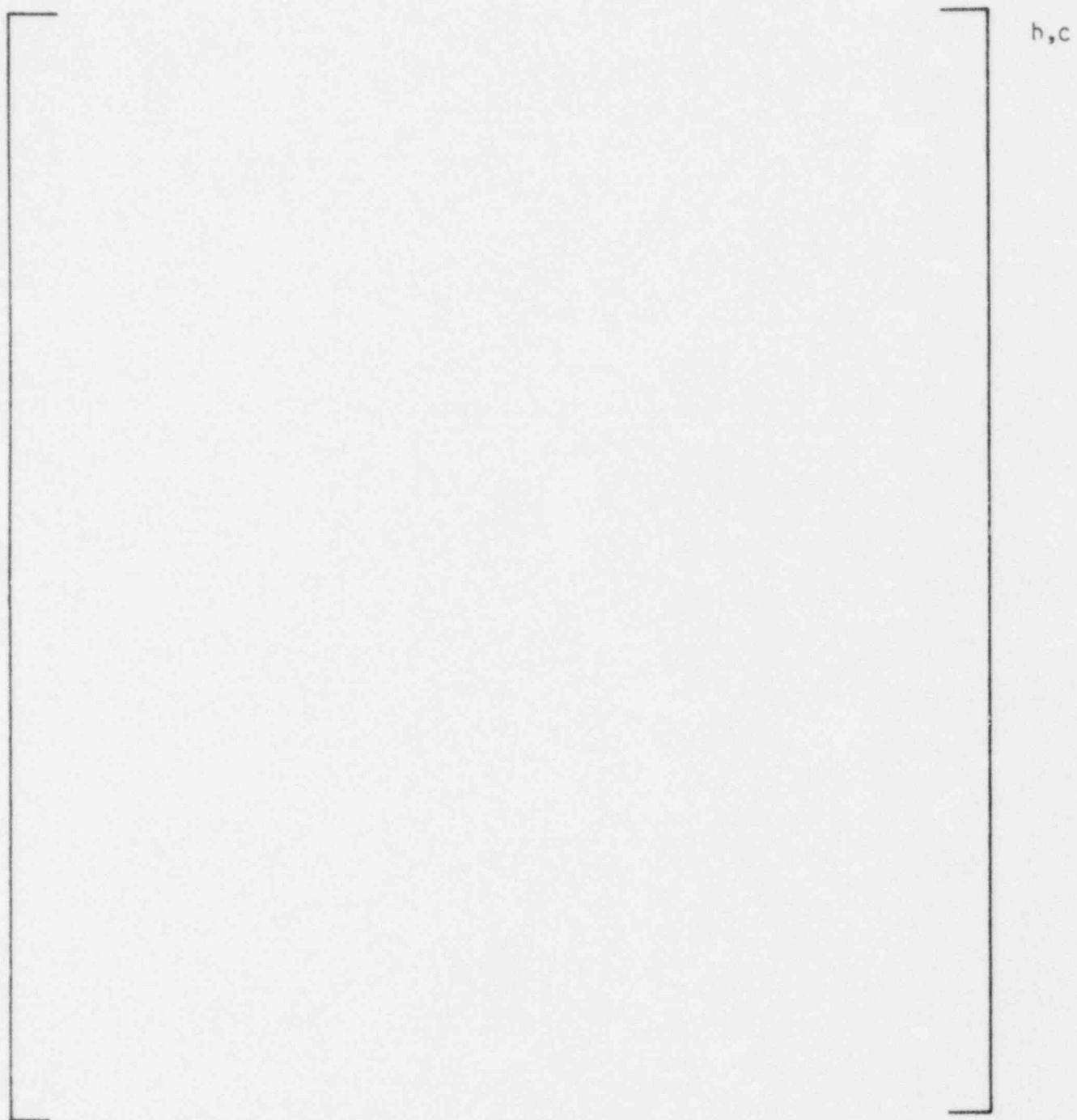


Figure 17-3. Total Vertical Force on Fuel Assembly C.G.

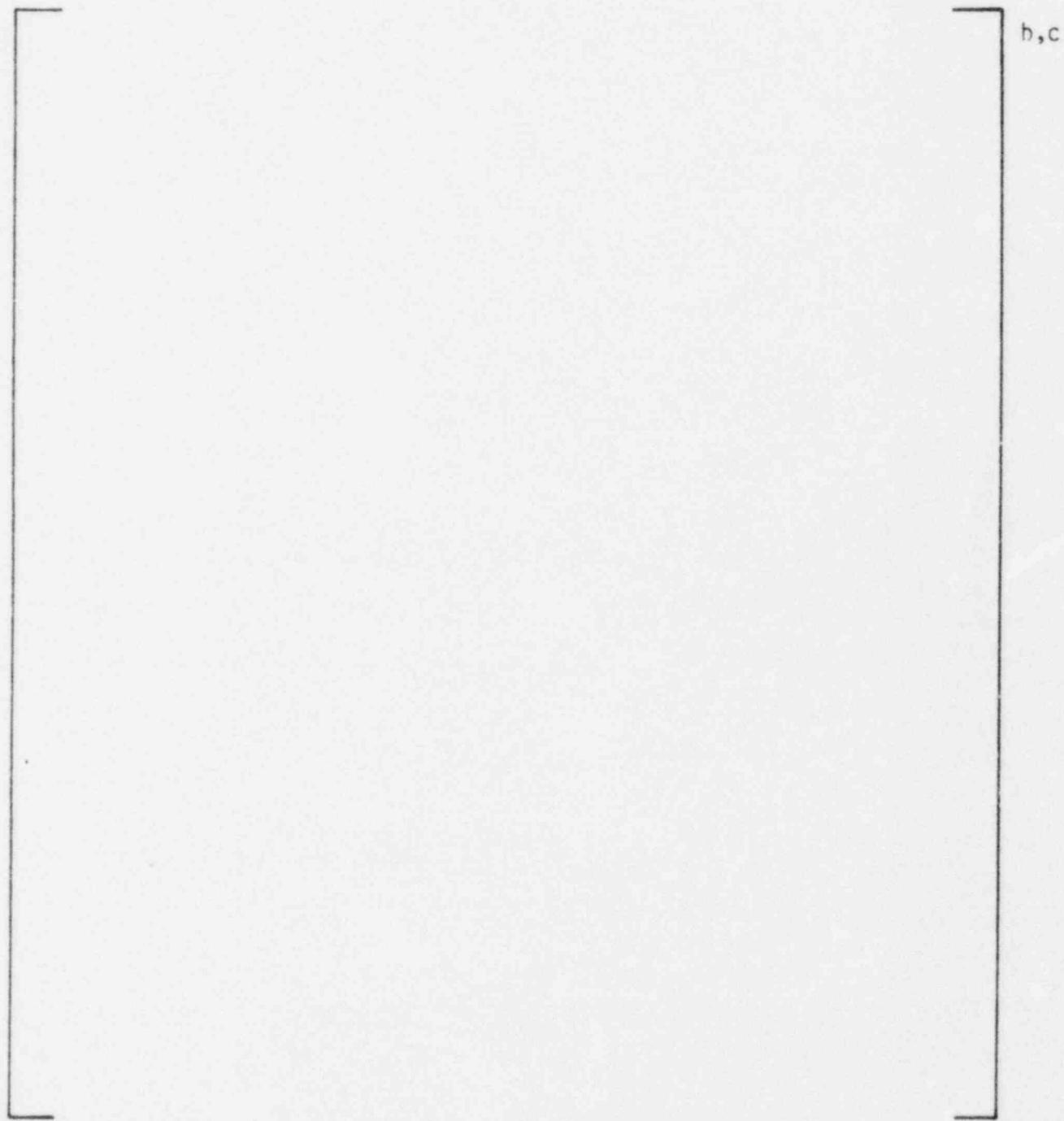


Figure 17-4. Total Vertical Force on Bottom Fuel Nozzle

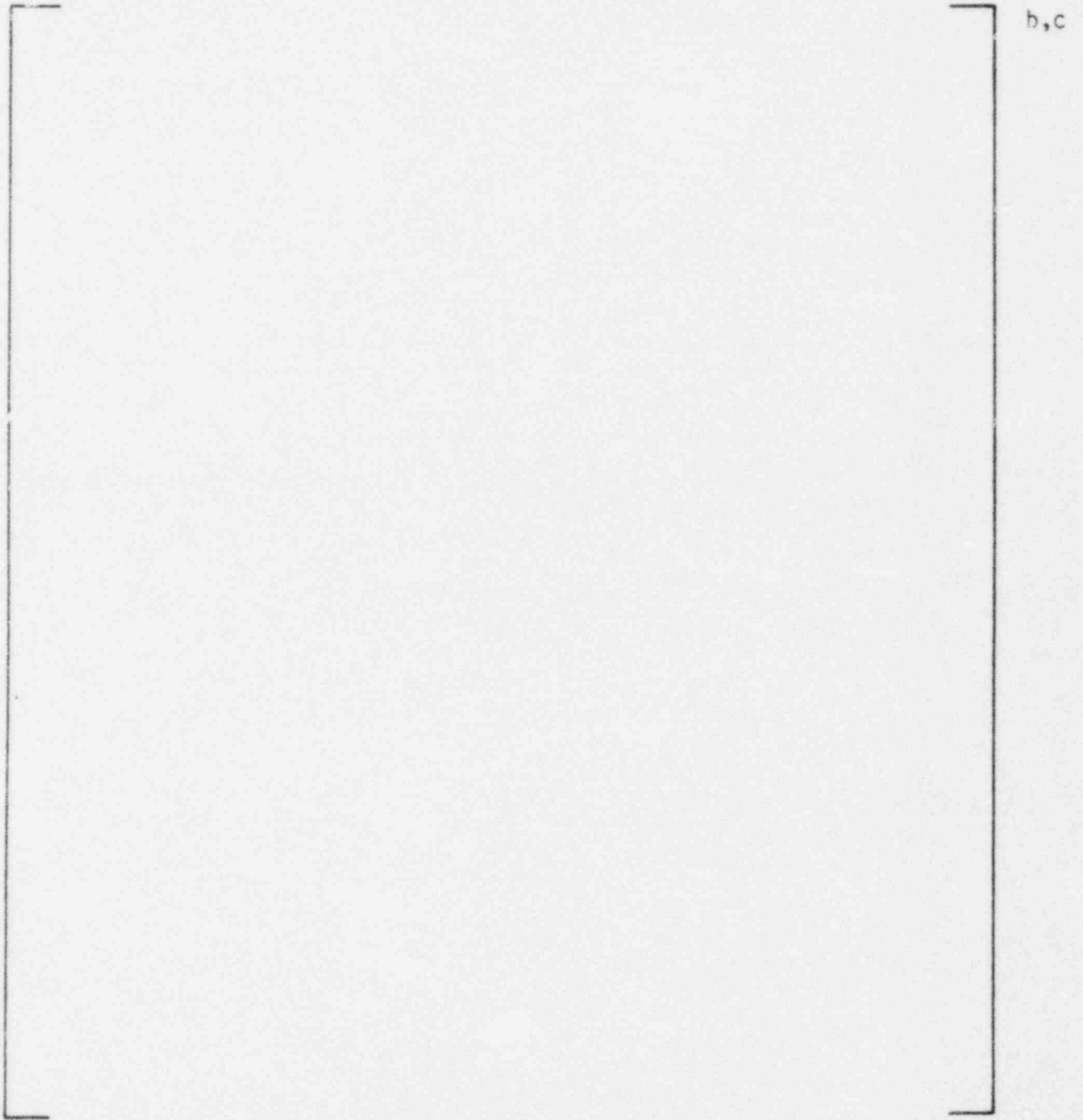


Figure 17-5. Total Vertical Force on Lower Core Plate

QUESTION 18 Table 3-7;

The maximum direct stress intensity for the guide thimble does not agree with the value presented in Table 3-6. Explain.

RESPONSE

The maximum direct stress value in Table 3-6 for guided thimble tube should read [ ]<sup>+</sup> instead of [ ]<sup>+</sup> which was a typographical error. a,c

QUESTION 19 Q1 question 3;

Combined motions in the horizontal and vertical direction were considered for beam-column effects in Reference 1. Has this type of assessment been performed for the optimized fuel assembly? If so, enclose the results. If not, why not? Explain.

RESPONSE

The beam-column effects were originally investigated in Ref. 1. The results of this study indicated that the higher order effects caused by the combination of axial and lateral deflections did not significantly alter the stress distribution. The test results as reported in Ref. 1 for an initially bowed assembly that was dropped from various heights indicated that the thimble stresses in the bowed assembly were slightly higher than those obtained for an initially straight assembly. Based on the fuel assembly axial impact tests as reported in Ref. 1, the effect of the fuel assembly bow resulted in an increase of approximately [ ]%<sup>+</sup> a,c in the maximum thimble stress. In view of the relatively large stress safety margin for the OFA design, the experimental and/or analytical investigations were not warranted.

\*Ref. 1. WCAP-8236.

QUESTION 20    General;

Review of the fuel assembly models requires the following additional information:

a. Masses

1. Fuel rod
2. Spacer grid
3. End nozzles
4. Guide and instrument tubes
5. Fuel column
6. Total fuel assembly and center of gravity

b. Other measured quantities

1. Axial gap between fuel nozzles and upper core plate
2. Axial hold down spring stiffness and preload.

RESPONSE a.

The dry weight distribution for the Optimized Fuel Assembly components are tabulated below:

		+
		a,b,c

The center of gravity of the fuel assembly is approximately located at the geometrical center.

RESPONSE b.

1. The axial gap between the top fuel nozzle and upper core plate =  
[       ]<sup>+</sup> in. a,c
2. Axial holddown spring stiffness = [       ]<sup>+</sup> lb/in. b,c  
Axial holddown spring preload = [       ]<sup>+</sup> lb. b,c

QUESTION 21      General;

An assessment of the combined SSE-LOCA transient event (including steady state conditions) is required. Provide component evaluations for this condition. Guidelines outlining acceptable response combination procedures are presented in References 2 and 3.

RESPONSE

The SSE and LOCA analyses presented in the topical report were treated independently and the results were not combined. The fuel assembly component stresses were obtained from the maximum fuel assembly relative deflection. Since the fuel assembly is displacement limited by the maximum accumulated gap clearances plus the grid deformations, the fuel assembly stresses presented in the report are basically a limit case.

Westinghouse has demonstrated that a simultaneous SSE and LOCA event is highly unlikely. The fatigue cycles, crack initiation and crack growth due to normal operating and seismic events will not realistically lead to a pipe rupture(\*). The factor applied to the LOCA grid impact load due to flashing is considered unrealistic since the thermal/hydraulic conditions for flashing are not present at the time of peak grid impact load. Nevertheless, the combined LOCA and SSE loads are supplied and the combined values are below the established limits, as summarized below.

The fuel assembly component stresses under the combined SSE/LOCA transients and the steady state operating loads (axial holddown spring preload and differential pressure loading) are summarized in Table Q21.1.

The combined maximum grid load responses based on the square-root-or-sum-of-squares is [      ]<sup>+</sup> lbs; and with the 1.3 factor on LOCA-load, the maximum combined grid load is [      ]<sup>+</sup> lbs.

(a,c)  
(a,c)

---

\* WCAP-9283

Table Q21.1

FUEL ASSEMBLY COMPONENT STRESSES AND LIMITS  
(ksi)

---

+

a, c

QUESTION 22    General;

Discuss control rod insertability for both the SSE and the SSE-LOCA transients.

RESPONSE

Under the SSE and SSE-LOCA transients, there will be no grid distortion or thimble buckling as a result of maximum grid impact and fuel assembly deflection responses. Thus the insertion of the flexible control rod will not be hindered. It should also be noted that the maximum grid impact response, in general, occurred at the peripheral fuel assemblies which do not contain control rod assemblies.

Question 23: Define the cavity pressure load cases considered. Include break locations, areas and opening times considered.

Response: Prior to performing the analyses presented in WCAP 9401, a series of LOCA analyses were performed to select a representative cavity pressure load case. The plants of concern were reviewed and available cavity loads collected to determine variations in the magnitude and transient nature of the cavity loads. In addition, cavity load cases from other Westinghouse plants not covered by WCAP 9401 which demonstrated unique transient characteristics were considered. The plants for which these cavity pressure loads apply have undergone US NRC licensing review. No open items exist for the methods used in the calculation of the cavity pressure loads. The effect of variation in cavity design, plant operating conditions and the distribution of applied cavity loads on the reactor vessel are reflected in the transient variation of the cavity loads considered.

Three cases were selected with distinctly different transient variations (Figures 23-1 through 23-9). These cases were all based on a 144 square inch reactor vessel inlet nozzle break with a break opening time of 1 millisecond. All three cases were ratioed so that the peak horizontal load was [ ]<sup>†</sup> This value is representative of (a,c) the peak horizontal cavity load applicable to any of the plants covered by WCAP 9401. Reactor vessel LOCA analyses were performed and fuel assembly impact loads were calculated for each of the three cases. The peak grid impact loads were [

] <sup>†</sup>

(a,c)

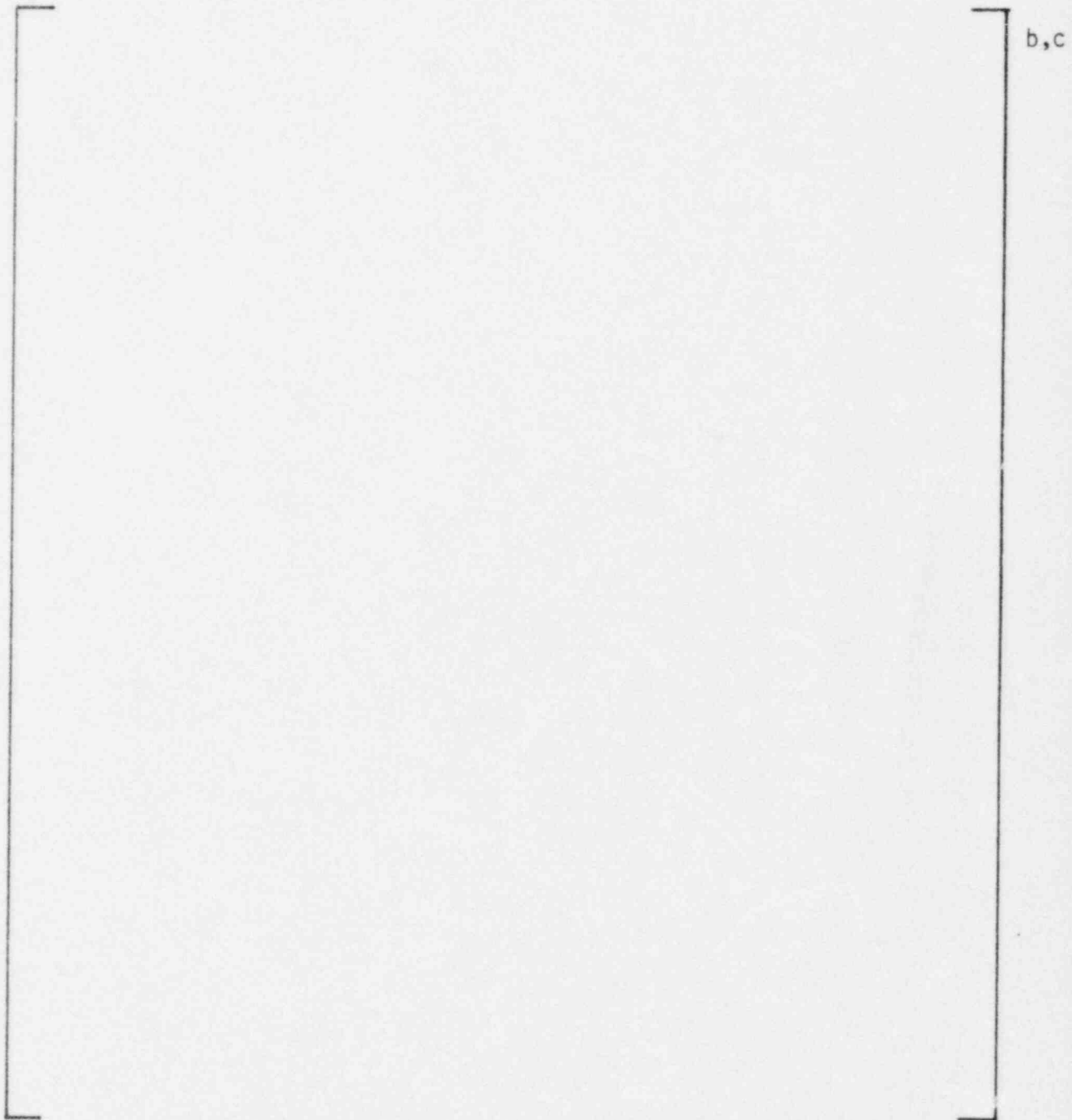


Figure 23-1. Cavity Load Case 1 Horizontal Force

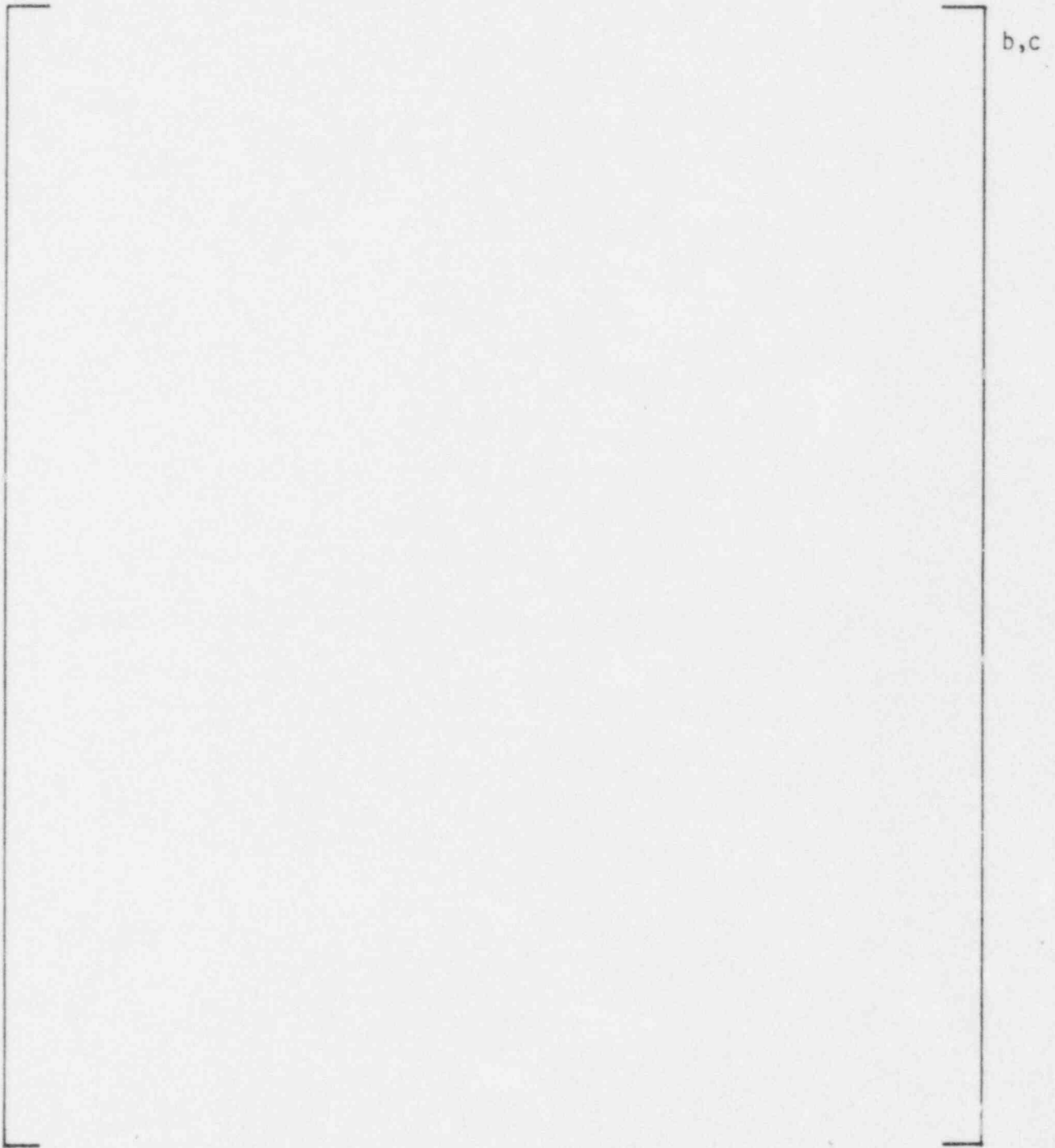


Figure 23-2. Cavity Load Case 1 Vertical Force

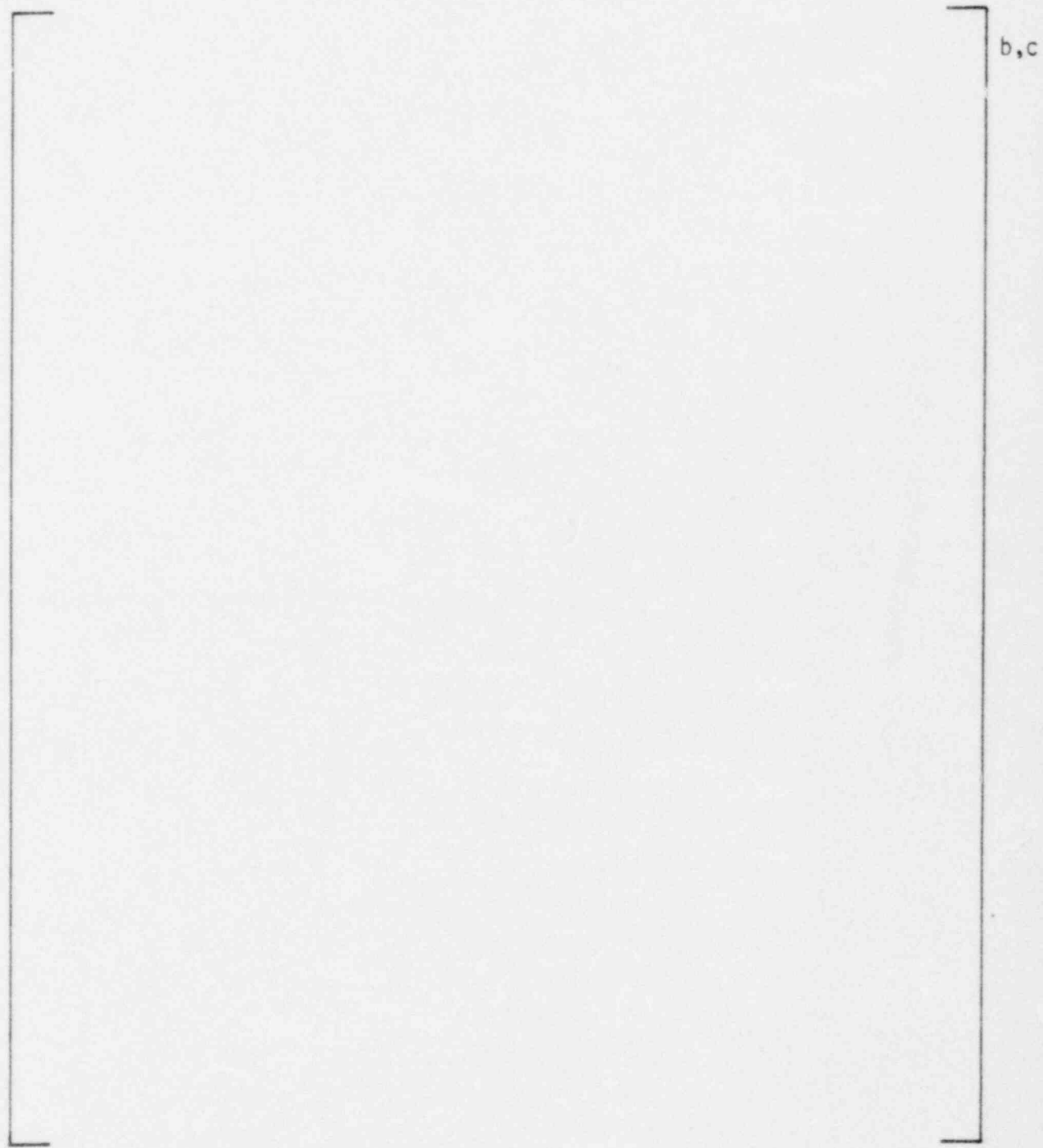


Figure 23-3. Cavity Load Case 1 Moment

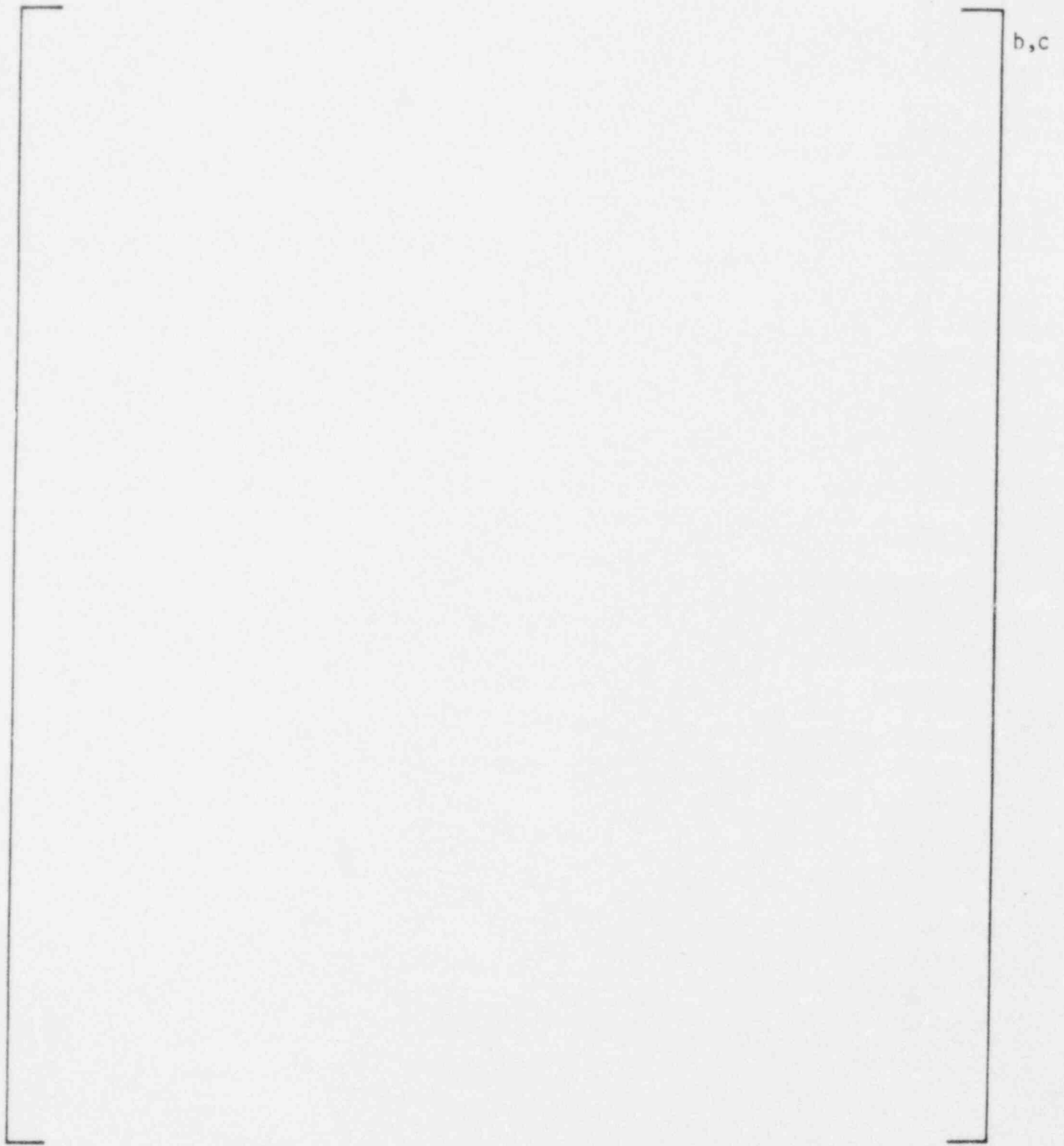


Figure 23-4. Cavity Load Case 2 Horizontal Force

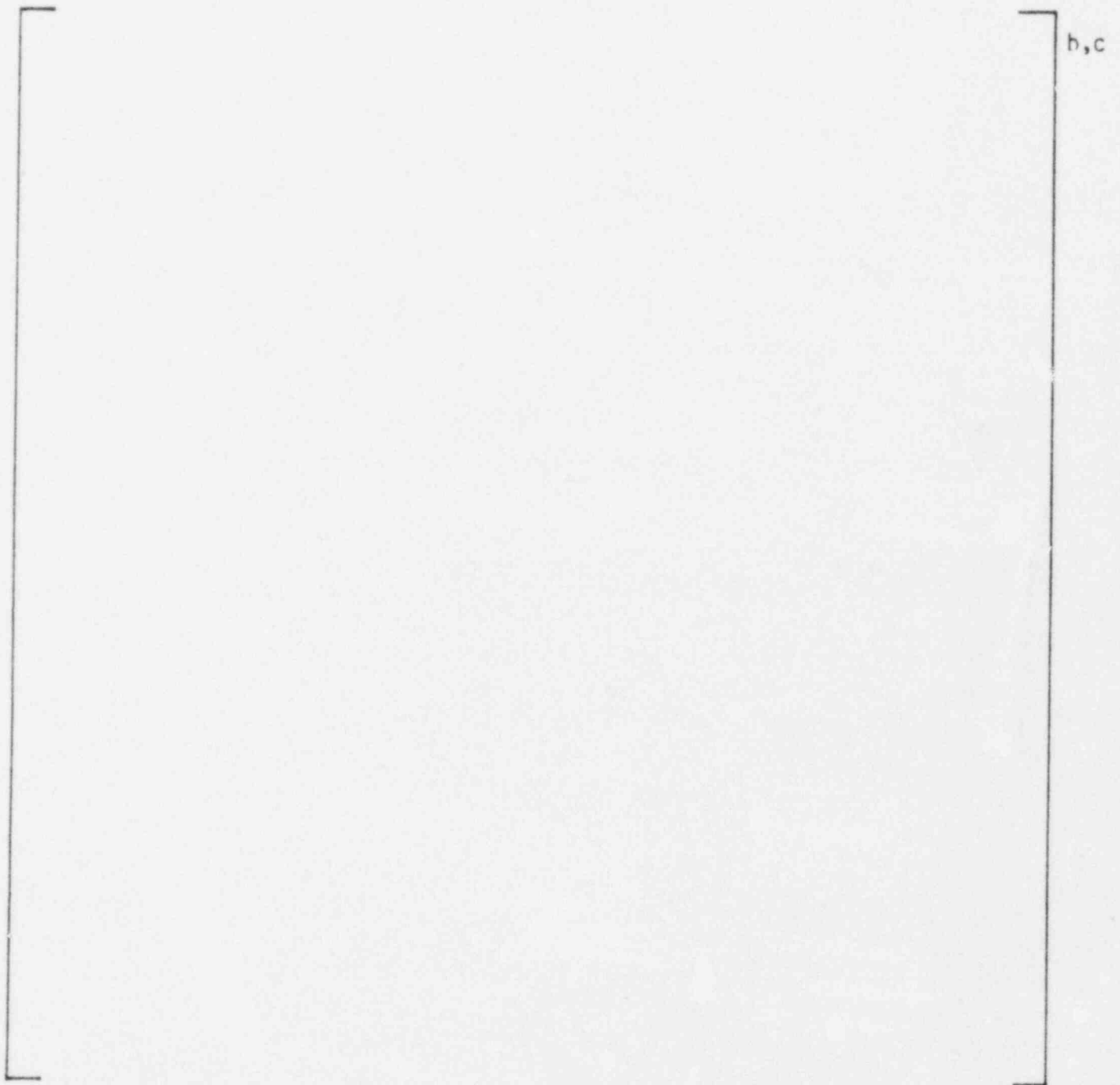


Figure 23-5. Cavity Load Case 2 Vertical Force

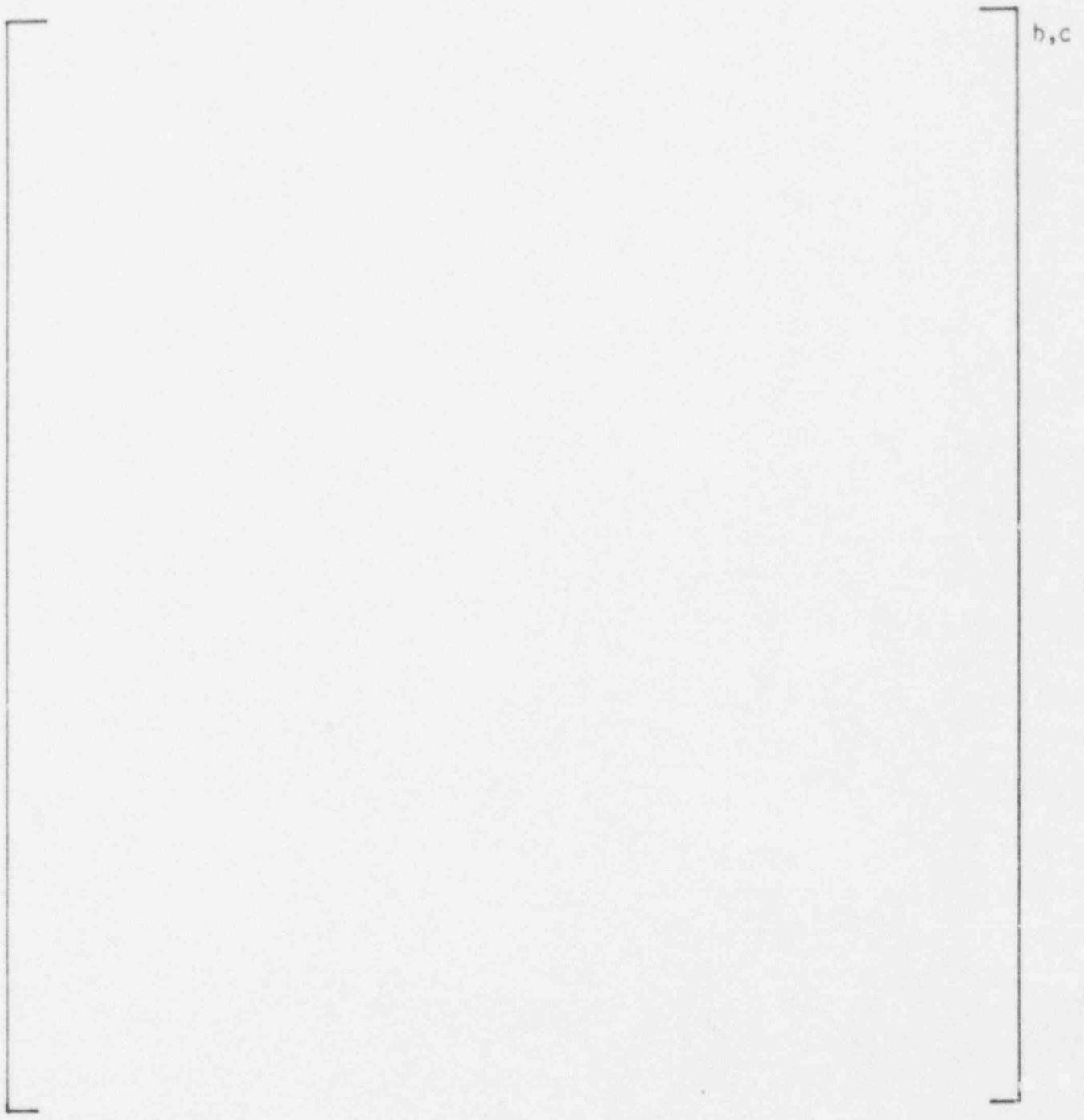


Figure 23-6. Cavity Load Case 2 Moment

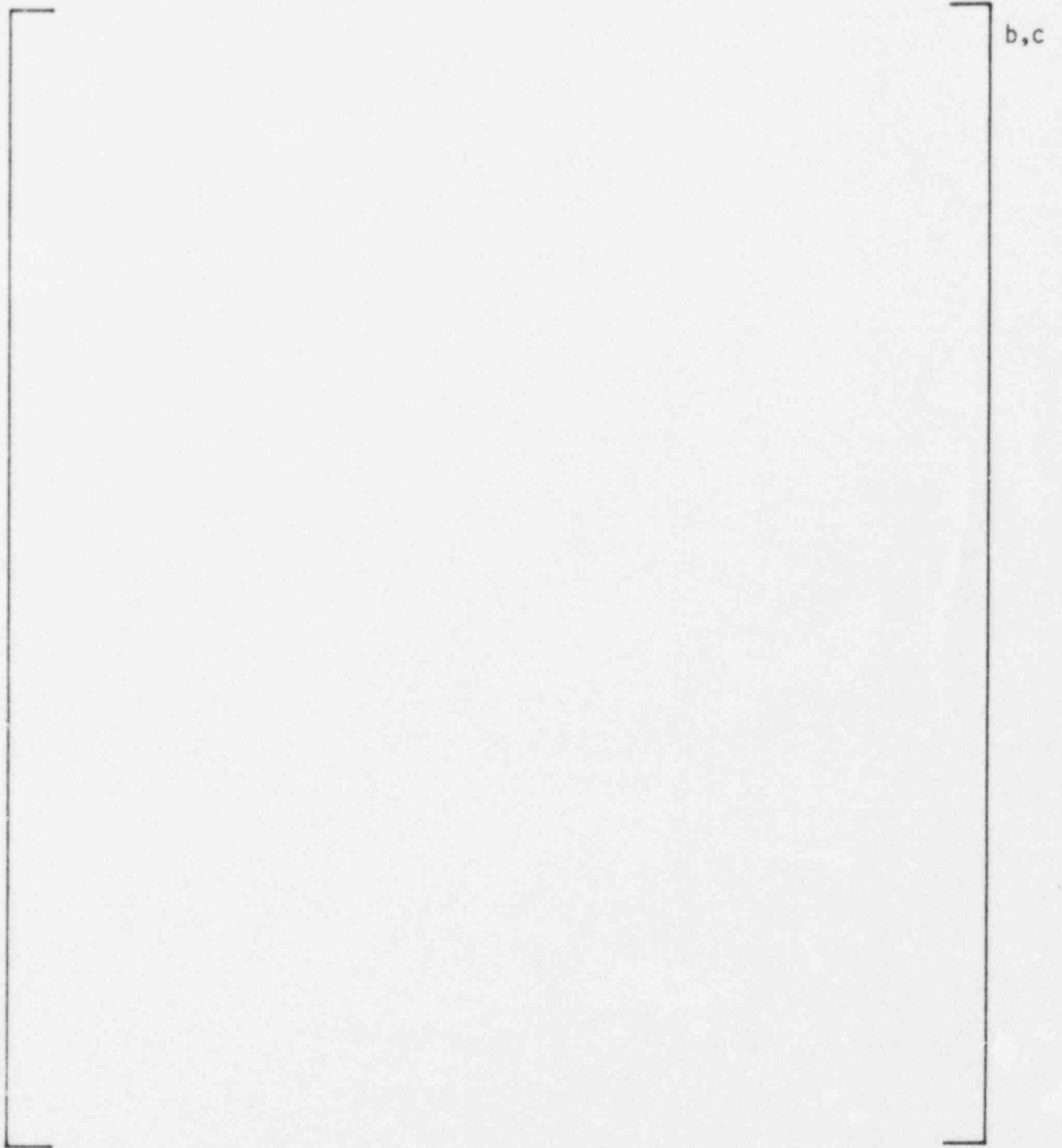


Figure 23-7. Cavity Load Case 3 Horizontal Force

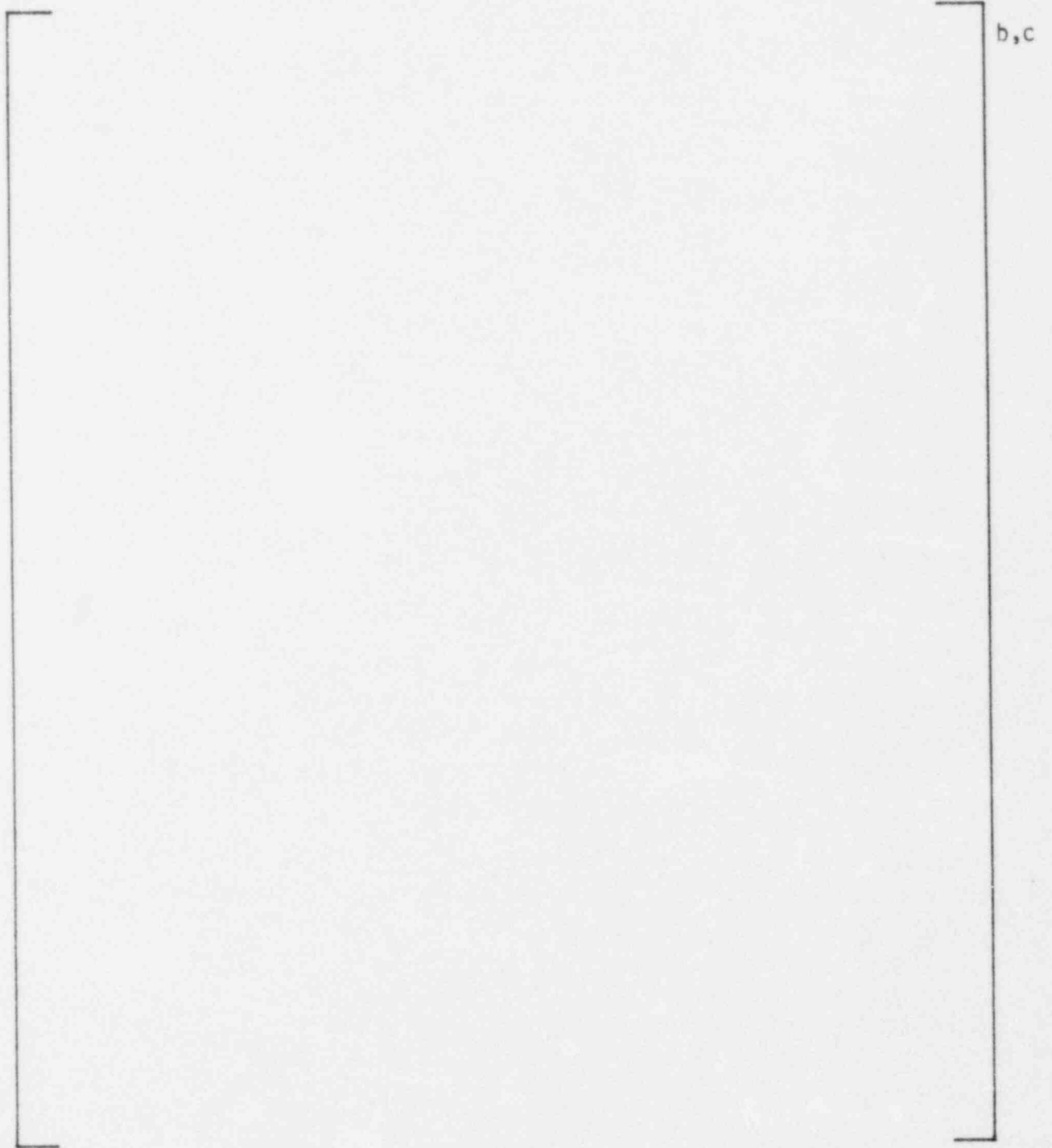


Figure 23-8. Cavity Load Case 3 Vertical Force

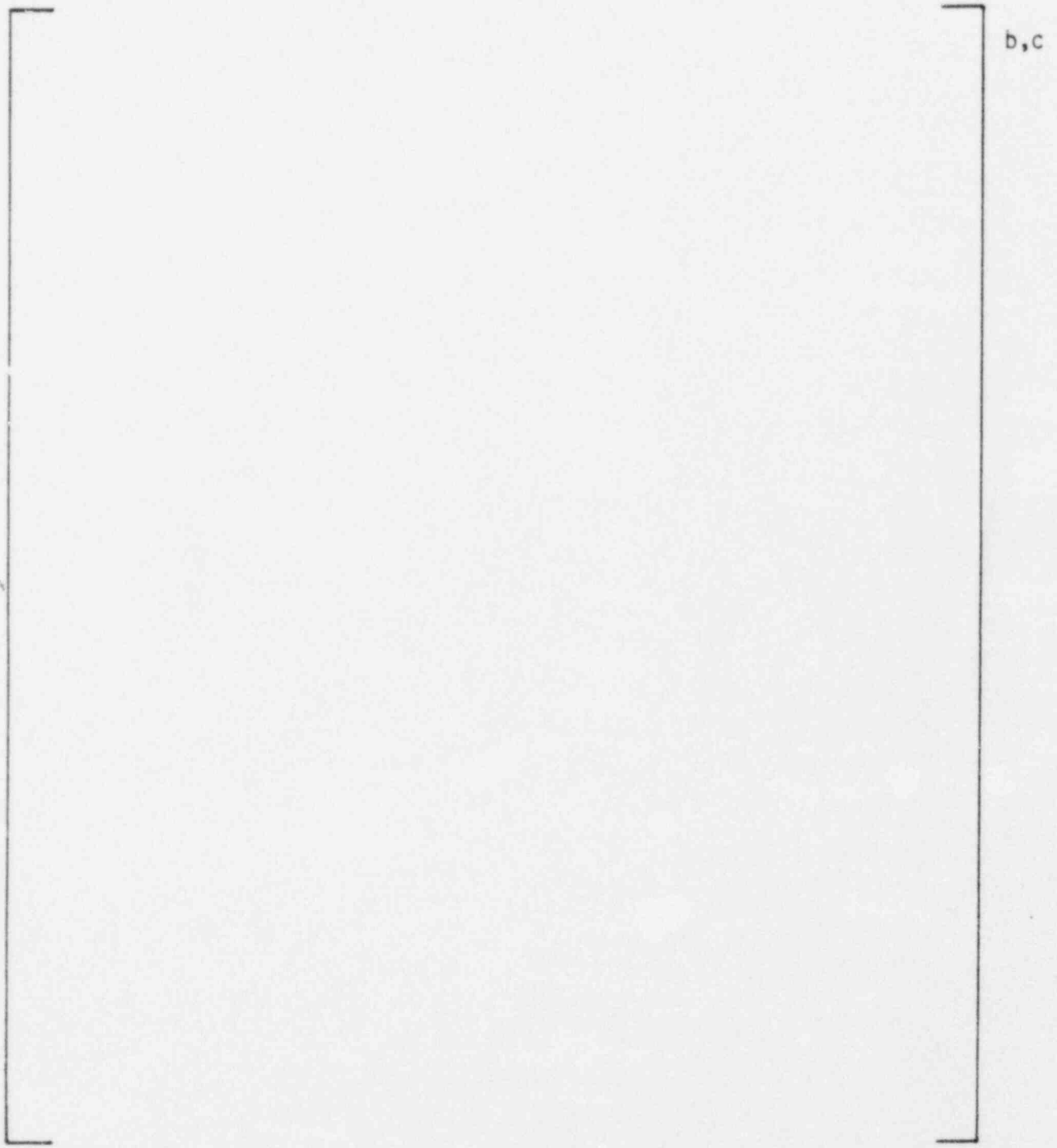


Figure 23-9. Cavity Load Case 3 Moment

## REFERENCES

1. Gesinski, L. T. and Chiang, D., "Safety Analysis of the 17x17 Fuel Assembly for Combined Seismic and Loss-of-Coolant Accident," WCAP-8236, December 1973.
2. Cudlin, R., et al., "Methodology for Combining Dynamic Responses," NUREG-0484, September 1978.
3. Standard Review Plan PSRP-4.2, proposed Appendix A "Evaluation of Fuel Assembly Structural Response to Externally Applied Forces."